

Evolution of deformation in the Buck Mountain Fault damage zone, Cambrian Flathead Sandstone, Teton Range, Wyoming

Stephanie R. FORSTNER, Stephen E. LAUBACH, András FALL

Bureau of Economic Geology, Jackson School of Geosciences, The University of Texas at Austin, Austin, Texas, U.S.A.
 E-mail: stephanie.forstner@beg.utexas.edu

The Teton Range is a normal fault block that contains older reverse faults (Love et al., 1992). Although generally considered to be Late Cretaceous to early Tertiary structures, the timing, kinematic style, and history of these faults is conjectural. Faults include the Forellen Peak Fault to the north, the Buck Mountain Reverse Fault (BMRF) to the west and south, and the Teton normal fault to the east (Love et al., 1992). The BMRF is rooted in Precambrian crystalline rocks and dips steeply to the east about 60°. The fractured Cambrian Flathead sandstone, an orthoquartzite (90%+ quartz), rests nonconformably on the Precambrian. Its stratigraphic position and relative isotropic mineralogy make the Flathead an ideal horizon for studying brittle deformation.

Oriented Flathead hand samples were collected from the footwall of the BMRF along a partially overturned syncline (Figure 1). Continuous SEM-Cathodoluminescence (SEM-CL) scanlines of these samples allow for a systematic kinematic analysis of the cemented opening-mode fractures. We quantify attributes such as; geometry, spacing, orientation, and cross-cutting relationships. In isotropic rock, mode-I fractures primarily propagate along the plane perpendicular to S_{hmin} ; therefore, microfractures can be used to indicate paleostress trajectories, strain, and relative fracture timing (Anders et al., 2014; Hooker et al. 2018). Since fracture cements appear synkinematic, we've determined the temperatures, pressures, and fluid compositions present during fracturing by conducting a high-resolution fluid inclusion assemblage (FIA) petrographic and microthermometric analysis. Our kinematic and geochemical analysis of diagenetic damage zone features provides spatial and temporal constraints on the conditions present during fracture development, the evolution of the local tectonics, and paleohydrology.

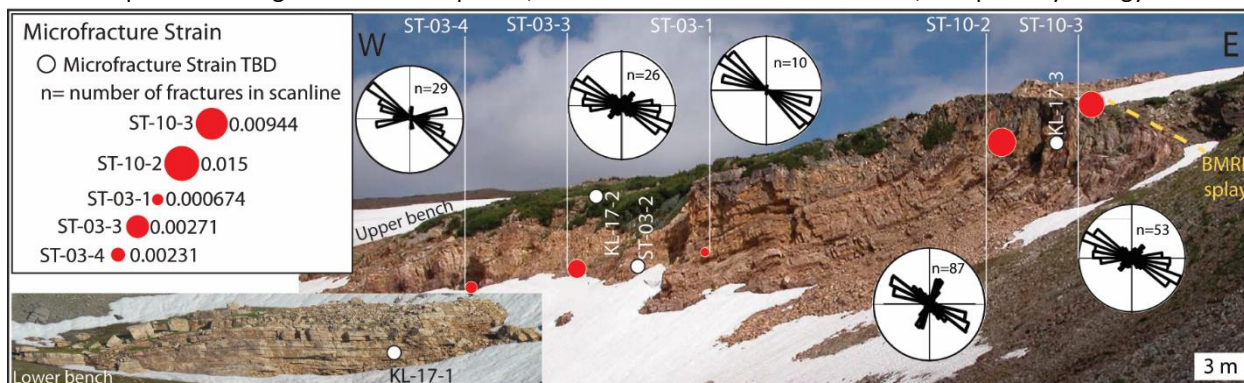


Figure 1: Flathead Sandstone syncline and fault at Kit Lake (43.716, -110.832). Sample locations, length-weighted fracture strike rose diagrams, and calculated total microfracture strain.

Steeply dipping fractures strike WNW, NW, and NE (Figure 1). In general, opening-mode fracture strain increases towards the fault and is highest near the fold axis. The strain calculation does not include the WNW and NE opening-mode fractures, prevalent nearest to the BMRF, which have undergone shear displacement. Fractures have opening displacements ranging from ~0.5 μ m to 3 mm. A few NW fractures contain quartz bridges and have preserved porosity. SEM-CL images of diagenetic cements reveal alternating light and dark luminescing textures; overgrowths are syntaxial and zoned whereas fractures contain wall-parallel crack-seal and wall-perpendicular fibrous textures, an indication of synkinematic cementation (Lander & Laubach, 2015). Fracture cements luminesce different colors under Color-SEM-CL, suggesting variation in fluid source and composition (Figure 2). Quartz overgrowths are crosscut by fractures and, therefore, formed early. The relative evolution of each brittle deformation period is supported by cross-cutting relationships and FIAs which reveal; WNW fractures formed first, followed by NW fractures, and lastly NE fractures.

The fluids present during overgrowth and fracture cementation are preserved in primary two-phase aqueous FIAs. Initial ice melting temperatures suggest cements precipitated from a H_2O -NaCl-CaCl₂(\pm MgCl₂)-type

fluid; however, only T_{mice} was observed. Therefore, we calculated salinity (expressed as wt% NaCl equivalent) assuming a H₂O-NaCl fluid model (Steele-MacInnis et al., 2012). Within petrographic context, minimum trapping temperatures (T_h) and salinity provide temporal

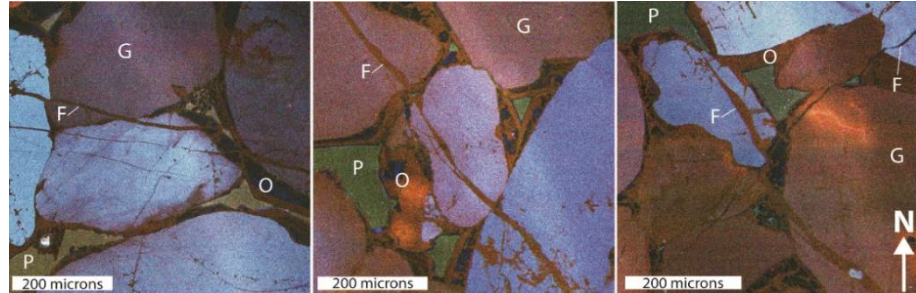


Figure 2: Color-SEM-CL images of WNW, NW, and NE striking fractures in sample ST-03-1A. G-grain; P-porosity; O-quartz overgrowth; F-fracture.

geochemical trends of deformation (Figure 3). Quartz overgrowths; T_h : 135-209°C and salinity: 4 to 7.5 wt.%. WNW-fractures; T_h : 140-170°C and salinity: 2.0-6.9 wt.%. NW fractures; T_h : 136-160°C and salinity: 11.7-13.5 wt.%. NE fractures; T_h : 110-191°C and salinity: 4.8-5.1 wt.%. On average, T_h ranges by 16.5°C within a single FIA.

Diagenetic cements precipitated from a wide range of fluid conditions. However, we can begin to temporally constrain fracture kinematics and fluid conditions present during diagenesis. Temperatures in quartz overgrowths show a heating trend which is compatible with progressive burial to maximum burial conditions. Cross-cutting relations and temperatures in fractures show a general cooling trend and suggest brittle deformation occurred after maximum burial, probably during uplift. Assuming fractures formed during tectonic shortening, orientations and cross-cutting relations suggest S_{Hmax} rotated from WNW to NW and finally to NE.

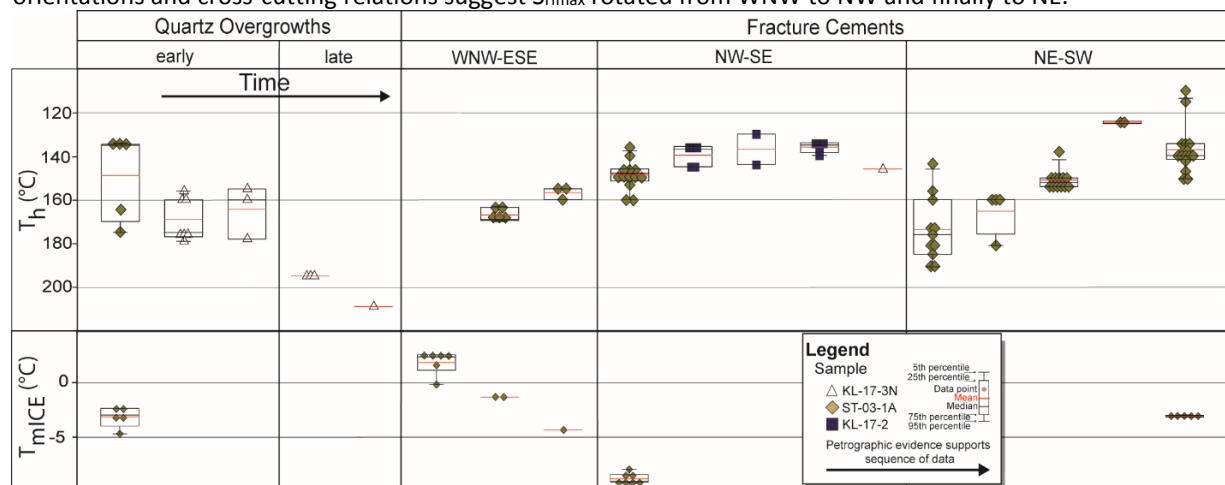


Figure 3: Fluid inclusion assemblage microthermometry results from quartz overgrowths and fractures. Cross-cutting relationships support the relative sequence (timing) of each diagenetic feature.

ACKNOWLEDGEMENTS

We are grateful to Grand Teton National Park for permission to sample under National Park Service permits GRTE-2014-SCI-0021 and GRTE-2017-SCI-0072.

REFERENCES

- Anders, M.H., Laubach, S.E., Scholz, C.H., 2014, Microfractures: a review. *J. Struct. Geol.* 69B, 377-394.
- Hooker, J.N., Laubach, S.E., Marrett, R., 2018, Microfracture spacing distributions and the evolution of fracture patterns in sandstones, *J. Struct. Geol.* 108, 66-79.
- Lander R.H., Laubach, S.E., 2015, Insights into rates of fracture growth and sealing from a model for quartz cementation in fractured sandstones. *Geol. Soc. Amer. Bull.* 127(3-4), 516-538.
- Love, J.D., Reed, J.C., Christiansen, A.C., 1992, Geologic map of Grand Teton National Park, Teton County, Wyoming; 1:62,500, USGS.
- Steele-MacInnis, M., Lecumberri-Sanchez, P., & Bodnar, R.J., 2012, HokieFlincs H₂O-NaCl: A Microsoft Excel spreadsheet for interpreting microthermometric data from fluid inclusions based on the PVTX properties of H₂O-NaCl, *Comp. Geosci.* 49, 334-337.